

## Development of a New Version of an Automatic Commutator Injector and a Procedure for the Photometric Determination of Ethanol in Distilled Spirits

Felisberto G. Santos<sup>a</sup> and Boaventura F. Reis<sup>\*,b</sup>

<sup>a</sup>Instituto de Química de São Carlos, Universidade de São Paulo,  
Av. Trabalhador São-carlense, 400, 13560-970 São Carlos-SP, Brazil

<sup>b</sup>Centro de Energia Nuclear na Agricultura, Universidade de São Paulo,  
Av. Centenário, 303, São Dimas, 13400-970 Piracicaba-SP, Brazil

Neste trabalho, uma nova versão de um injetor automático, mantendo a geometria retangular, é apresentada. Um pequeno motor de corrente contínua foi utilizado para realizar o deslocamento da parte central. A eficácia do injetor foi comprovada através do desenvolvimento de um procedimento para a determinação fotométrica de etanol em bebidas destiladas baseado na reação com dicromato em meio ácido sulfúrico e detecção fotométrica usando um LED como fonte de emissão em 590 nm. O sistema mostrou bom desempenho analítico, simplicidade de operação e versatilidade, incluindo também as seguintes características: resposta linear ( $r = 0,9972$ ) para a faixa de concentração de 10 a 50% (v/v) de etanol, limite de detecção de 2,0% (v/v) de etanol, desvio padrão relativo de 2,0% ( $n = 10$ ) para uma amostra com concentração de etanol de 40% (v/v), consumos de 5,8 mg de  $K_2Cr_2O_7$  e 198  $\mu$ L de  $H_2SO_4$ , e geração de 0,73 mL de efluentes por determinação.

In this work, a new version of an automatic injector is proposed, keeping the rectangular geometry. In this version, a small DC motor was employed to perform the displacement of the central part. The effectiveness of the injector was confirmed through the development of a procedure for the photometric determination of ethanol in distilled spirits based on the reaction with dichromate in a sulfuric acid medium and photometric detection using an LED based photometer. The system demonstrated the best analytical performance, versatility and simplicity of operation, also including the following features: linear response ( $r = 0.9972$ ) for the concentration range of 10 to 50% (v/v) ethanol, 2.0% for the limit of detection (v/v) of ethanol, a relative standard deviation of 2.0% ( $n = 10$ ) for a sample with an ethanol concentration of 40% (v/v),  $K_2Cr_2O_7$  and  $H_2SO_4$  consumptions of 5.8 mg and 198  $\mu$ L, respectively, and effluent generation of 0.73 mL per determination.

**Keywords:** flow injection analysis, automatic injector commutator, ethanol in distilled spirits, multicommutation, LED photometer

### Introduction

Since the initial proposal presented by Ruzicka and Hansen<sup>1</sup> in 1975, the flow injection analysis (FIA) process has always been linked to the means employed to introduce the sample aliquot into the analytical path. In early work, the aliquot of a sample solution was inserted into the analytical path using a hypodermic needle, which was done by piercing a rubber septum. After a few injections, leaking of solution occurred through the septum, requiring interruption of the work to replace it. This deficiency was

overcome when an injector that did not require the use of needle was proposed.<sup>2</sup> In this new device, a rubber septum acted as a valve, which gave way under external pressure exerted on the syringe plunger, releasing the channel that gave access to the analytical path. With this new device, the FIA process became more robust, but it still had some drawbacks. The precision of the measurements depended on the constancy of the injection time, thus requiring a well-trained operator. This problem had been overcome with the invention of the rotary valve by Ruzicka *et al.*,<sup>3</sup> and the proportional injector by Bergamin *et al.*<sup>4</sup> With the rotary valve, the volume of the sample aliquot was defined by a transverse hole made in the rotor.

\*e-mail: reis@cena.usp.br

The proportional injector comprised three pieces generally machined in acrylic and attached together with screws. The central part can be displaced in relation to the two sides, thus commuting all sections of the injector between two fixed states. The volume of the sample aliquot was defined by the length and internal diameter of the sampling loop. Therefore, variations in the sample volume to be inserted into the analytical path could be easily performed by exchanging the sampling loop. This device afforded great flexibility to the FIA process since the replacement of the sampling loop could be carried out without causing any disturbance in the flow system. The commutator injector of rectangular geometry has been preferred to the development of automatic analytical procedures.<sup>5</sup> In this case, the central bar has been displaced by using a pair of solenoids or a stepper motor.<sup>6,7</sup>

In this work, a new version of the commutator injector based on the rectangular geometry and maintaining the usual configuration of three pieces is presented. On the inside of the two side pieces, channels (3 mm deep and 12 mm wide) were machined where the central part was fitted. In this condition, the adjusting screws do not function as a guide, the case for the first-generation injector. This design facilitated the replacement of the movable part and contributed to reducing the friction, thereby allowing the use of a small DC motor to move the central piece from the sampling position to the injection position and *vice versa*.

Intending to demonstrate the feasibility of this new version, the injector was employed in the development of an analytical procedure for the photometric determination of ethanol in distilled spirits. The procedure was developed using the reaction of ethanol with dichromate in a sulfuric acid medium.<sup>8,9</sup> The work is focused on low reagent consumption and reduction of effluent generation. Whereby, in order to accomplish these requirements, the flow analysis module comprised an automatic injector and a set of solenoid valves, which were assembled to work as independent flow line commuting devices, according to the multicommutation process.<sup>10-12</sup> The photometric detection system was designed to use a LED as a source of electromagnetic radiation and a photodiode as a signal transducer, comprising an arrangement similar to those employed in other works.<sup>13,14</sup>

## Experimental

### Reagents and solutions

All solutions were prepared with purified water with an electric conductivity less than  $0.1 \mu\text{S m cm}^{-1}$ . All chemicals were analytical grade reagents.

A  $0.2 \text{ mol L}^{-1} \text{ K}_2\text{Cr}_2\text{O}_7$  (Merck) solution was prepared in a  $4.0 \text{ mol L}^{-1}$  sulfuric acid medium by dissolving 5.8838 g of solid in 22.0 mL of concentrated acid. After dissolution, the content was added slowly to a glass vessel containing 50 mL of water under continuous mixing. The volume was made up to 100 mL with water. Reference solutions with concentrations of 0.0, 10.0, 20.0, 30.0, 40.0 and 50.0% (v/v) ethanol were prepared daily from a stock of 99.9% absolute ethanol (Merck) using water as the diluent. Samples of *cachaça*, whisky and vodka were obtained from a local market.

### Apparatus and accessories

The equipment setup and accessories used in the current work included an IPC8 Ismatec peristaltic pump equipped with Tygon pumping tubes of different inner diameters; a microcomputer equipped with an electronic interface card PCL711 (Advantech) and running a software written in Quick Basic 4.5; acrylic plates with thicknesses of 12 and 25 mm for construction of the automatic commutator injector; two three-way solenoid valves (HP225T031, NRResearch) and two pinch solenoid valves (225P091-11, NRResearch); a DC motor (Microred R-Vdc) with speed reducer to 17 rpm, working voltage of 12 V, current intensity of 0.4 A and torque of 16 N cm; a stabilized power supply (12 V DC, current intensity of 2 A) to feed the solenoid valves and the DC motor; a stabilized power supply of +12 V and -12 V (0.5 A) used to feed the photometer; four relays of 12 V and contact current of 10 A; two push-button electric switches with sliding rod (VT16051C2, Higly), contact current of 15 A; four BC547 transistors; a power digital interface based on the integrated circuit ULN2803; a slotted optical switch (OPB866T55); three printed circuit boards, dimensions  $10 \times 20 \text{ cm}$ , in fiberglass with universal type drilling island to integrated circuit; a high-intensity emission LED with maximum at 590 nm; an OPT301 photodetector (Burr-Brown); a Z-format flow cell molded using a boron-silicate glass tube; a brass screw machined with the required features (trapezoidal thread of  $4.0 \text{ mm per turn}$ , diameter of 15 mm, length of 5 cm and central lead hole at one end to fit the motor shaft); an aluminum plate 8 cm wide, 10 cm high and 2 cm thick that has a threaded hole in the center (female) with the same dimensions as the screw; a laboratory densimeter model 4500M DMA (Anton Paar); and reaction coils and flow lines of polyethylene tubing with an 0.8 mm inner diameter.

### Detailed description of the injector

Figure 1 shows a three-dimensional view of the commutator injector ready to be used. The channels (cm)

machined on the internal faces of the side pieces allow the fitting of the central piece.

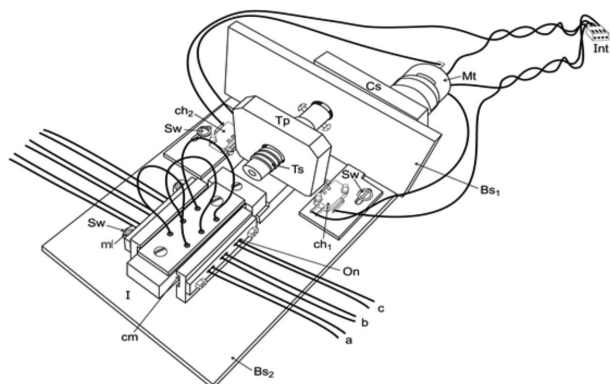


**Figure 1.** Three-dimensional view of the injector. Mt = DC motor; Cs = gearbox for rotation reduction; Sw = screws; Tp = traction plate; Ts = traction screw, 15 mm diameter, with trapezoidal thread, 4.0 mm *per* turn; ch<sub>1</sub> and ch<sub>2</sub> = electric switches with sliding rod; mt = springs; cm = channels for fitting the movable part; Bs<sub>1</sub> = DC motor holding, aluminum plate, 100 × 80 × 15 mm; Bs<sub>2</sub> = backing plate (PVC), surface of 25 × 40 cm and 25 mm thick; I = injector, a, b = polyethylene tubing flow lines, internal diameter of 0.8 mm; On = rubber O-ring seals; Int = interface for DC motor driving (Figure 2).

Sampling loops and tubes used as solution conduits through the injector were fixed with rubber O-rings in order to avoid the use of glue. Silicon rubber strips (4 mm wide and 2 mm thick) were glued onto the movable part of the injector to prevent internal leakage of fluids, and also to minimize friction. The strips of rubber were lubricated with silicon grease. The switches ch<sub>1</sub> and ch<sub>2</sub> defined the displacement of the mobile part. When the motor was driven, the traction plate (Tp) was displaced forward or backward depending on the direction of the DC motor rotation, thus displacing along with it the movable part of the injector. The switches ch<sub>1</sub> and ch<sub>2</sub> were assembled in order to open the electric circuit of the DC motor when the internal ducts of the injector were aligned. Under these conditions, the selected solution flowed through the injector.

Figure 2 shows the electric circuit of the control interface, which allowed the DC motor to switching on and off and set the direction of rotation using only two control bits (d<sub>6</sub> and d<sub>7</sub>).

In this configuration, when bit d<sub>7</sub> was turned on, transistor Tr<sub>2</sub> closed the electric circuit constituted by the relays R<sub>1</sub>, R<sub>2</sub> and the DC motor, which rotated clockwise. When the movable part of the injector (see Figure 1) reached the alignment position, the traction plate (Pt, Figure 2) pressed the sliding rod of switch ch<sub>1</sub>, which opened the electric circuit. After a predetermined time interval to fill the sampling loop, bit d<sub>6</sub> was activated and closed the electrical circuit that comprised transistor Tr<sub>1</sub>, relays R<sub>3</sub> and R<sub>4</sub>, and the DC motor, which rotated in a

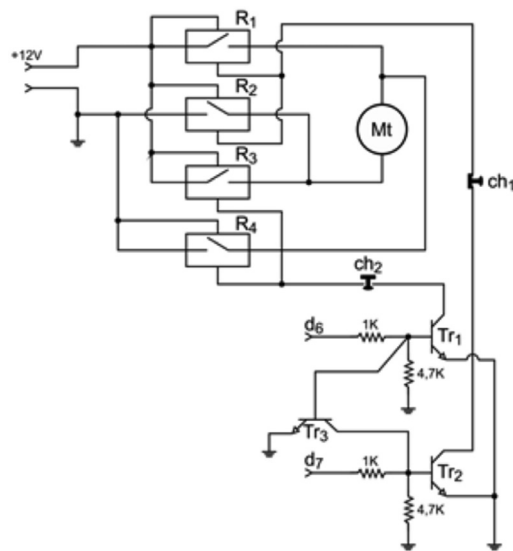


**Figure 2.** Diagram of the motor control interface. Mt = DC motor, R<sub>1</sub>, R<sub>2</sub>, R<sub>3</sub> and R<sub>4</sub> = relays; Tr<sub>1</sub>, Tr<sub>2</sub> and Tr<sub>3</sub> = transistor, BC547; ch<sub>1</sub> and ch<sub>2</sub> = electrical switches with sliding rod, d<sub>6</sub> and d<sub>7</sub> = control bits from the PCL711 interface card.

counterclockwise direction. In this condition, the mobile part of the injector was moved towards the injection position, and when it attained the alignment position, the switch ch<sub>2</sub> opened the circuit, and stopped the motor.

Transistor Tr<sub>3</sub> was installed to avoid conflict of duplicity, so that if both control bits are activated simultaneously, Tr<sub>3</sub> disables transistor Tr<sub>2</sub> by maintaining its base at a low level of electric potential difference (< 0.8 V). In this condition, the relays R<sub>3</sub> and R<sub>4</sub> were switched on and the motor rotated in counterclockwise.

The diagram of the photometer constructed for this study is shown in Figure 3, which consists of three main parts: a radiation source comprising a LED of high brightness, a transistor and resistors; a flow cell and its support; and a photodiode (OPT301). This photodetector was included in the same package circuits to convert radiant energy to electric current and to perform signal amplification, thus exempting the need for any circuit for additional signal amplification.

The intensity of the radiation beam was a function of the electric current intensity flowing through the LED, which was controlled by the variable resistor (10 kW) coupled to the base of the transistor (Tr). The radiation beam (I<sub>a</sub>) emitted by the LED propagated through the flow cell and emerged at the other end, reaching the photodetector (Det). When the flow cell was filled with a solution that absorbed radiation in the same range of wavelength emitted by the LED, absorption occurred during the radiation propagation, thereby causing an attenuation of the beam intensity. As a result, the radiation beam (I<sub>b</sub>) reaching the detector was less intense than the initial one (I<sub>a</sub> > I<sub>b</sub>). The variation of

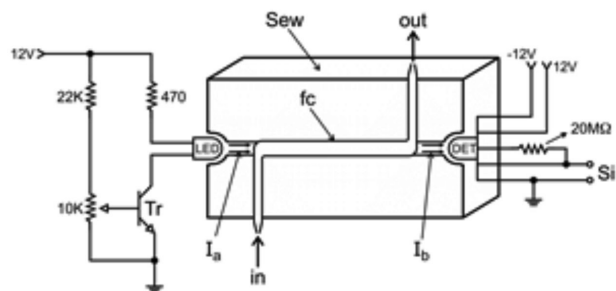


**Figure 3.** Diagram of the photometer. Sew = sectional view of the acrylic plate used as a assembling bracket for the photometer; Tr = transistor BC547, LED = light emitting diode,  $\lambda = 590$  nm, fc = flow cell body, glass tube (boron-silicate), 50 mm long and 1.2 mm internal diameter;  $I_a$  and  $I_b$  = radiation beams emitted by the LED entering and exiting the flow cell, respectively; Det = photodetector OPT301; in and out = fluid input and output, respectively; Si = signal generated by the photometer (mV).

the intensity ( $DI = I_a - I_b$ ) was a function of the chemical species present in the flow cell. The photometric detector transformed the variation in intensity of the light beam into a difference of electric potential (mV), which was used as a parameter in order to determine the concentration of the chemical species.

#### Operation description of the analysis module

Intending to demonstrate the feasibility of this new version of the commutator injector, the device was employed to assemble a flow analysis module to be used in the development of a procedure for the photometric determination of ethanol in distilled spirits. Since the ethanol concentration in the distilled spirits to be analyzed was very high, the flow system module was designed with ability to accomplish on line dilutions, which was done by implementing the sampling zone strategy.<sup>15,16</sup>

The diagram of the manifold is shown in Figure 4, and in this configuration, the injector is in the sampling position and all valves are turned off. The fluids including water and solutions of sulfuric acid and potassium dichromate ( $R_1$ ,  $R_2$ ) are being pumped towards the respective reservoirs.

When the control and data acquisition software was run, the first activity performed was the displacement of the injector to the sampling position as shown in Figure 4, which was done by activating control bit ( $d_7$ ) (Figure 2). Afterwards, by switching on valve  $V_1$ , the sample was aspirated through the sampling loop ( $L_1$ ). After a preset time interval ( $\Delta t_1$ ), the valve was turned off, and control bit  $d_6$  (Figure 2) was activated to start the DC motor in order to displace the injector towards the injection position (dilution), which is indicated in Figure 4 by the shaded surface. In this position, the resampling ( $L_2$ ) was included in the carrier fluid pathway (water). Valve  $V_4$  was switched

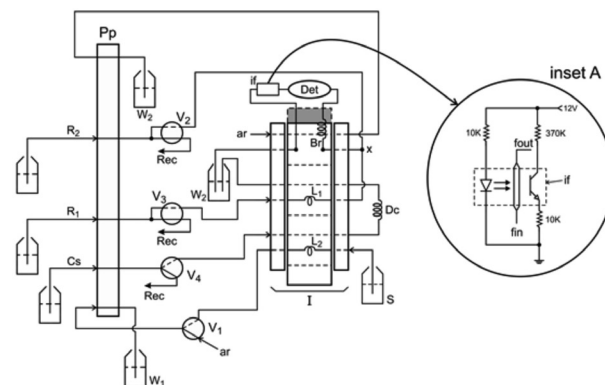


**Figure 4.** Diagram of the flow system manifold.  $V_1$  and  $V_4$  = three-way solenoid valves,  $V_2$  and  $V_3$  = solenoid pinch valves; Pp = peristaltic pump, I = automatic injector commutator, Br = reaction coil, 48 cm long and 0.8 mm inner diameter; Cs = carrier fluid (water), flow rate at 2 mL  $\text{min}^{-1}$ ;  $R_2$  and  $R_1$  = sulfuric acid and potassium dichromate solutions, flow rates of 2 and 1 mL  $\text{min}^{-1}$ , respectively; Rec = solution recirculation; Dc = dilution coil, 20 cm long, 0.8 mm inner diameter;  $L_1$  and  $L_2$  = sampling and resampling loops, respectively, inner volume of 50  $\mu\text{L}$ ; S = sample, flow at 2 mL  $\text{min}^{-1}$ ; Det = photometer,  $\lambda = 590$  nm; X = flow lines joint device; ar = air stream, flow rate at 2.5  $\text{min}^{-1}$ ;  $W_1$  and  $W_2$  = wastes; If = infrared detection, Inset A; fin and fout = fluid input and output, respectively. The arrows indicated the pumping direction. The shaded surface indicated the other commuting position of the injector. Dashed and solid lines in the valve symbols indicated the fluid pathway when the valves were switched on or off, respectively.

on in order to direct the water stream through the sampling loop ( $L_1$ ), thus displacing the sample aliquot through the dispersing coil (Dc) and the resampling loop ( $L_2$ ) towards the waste (Desc<sub>2</sub>). During displacement, the sample aliquot was dispersed into the carrier fluid (Cs), and therefore, the concentration of ethanol in the portion of the sample zone contained in the resampling loop ( $L_2$ ) varied with the time interval ( $\Delta t_2$ ). While the injector remained in the position of dilution (shaded surface), the air stream flowed by suction through coil  $B_1$  and the flow cell, emptying them completely. After the time interval ( $\Delta t_2$ ), valve  $V_4$  was switched off, and the mobile part of the injector was moved to the sampling position, shown in Figure 4. Afterwards, valves  $V_2$  and  $V_3$  were switched on and off alternately in order to insert aliquots of chromogenic reagent ( $R_2$ ) and sulfuric acid ( $R_1$ ) solutions, respectively. Under this condition, the sample aliquot was displaced from the loop  $L_2$  through reaction coil Br towards the photometer (Det), and the aliquot of reagents  $R_2$  was added at the joint device (X). Time intervals to maintain the solenoid valves  $V_2$  and  $V_3$  switched on or off were maintained at 1.0 s. While inserting reagent progressed, the microcomputer read the signal generated by the detector of infrared radiation comprised by the inset A in Figure 4. The flow cell, reaction coil (Br) and flow cell outlet tube were emptied in the preceding step, and under this condition, the signal generated by the infrared detector (If) was approximately 50 mV. When the sensing tube was filled

with sample solution, the signal magnitude was threefold. When the microcomputer detected this jump of signal, it shut down valves  $V_2$  and  $V_3$  and performed the signal reading step. While the reading step proceeded, valve  $V_1$  was kept switched on to fill the sampling loop ( $L_1$ ) to be used in the next analytical run. This sequence of events was performed automatically by the microcomputer, and it is summarized in Table 1.

Steps 1 to 4 were performed only one time, when the system operation began. Step 5 was performed whenever a new sample was processed, and steps 6 to 12 were executed sequentially to carry out each replicate. The photometer calibration (step 4) was performed following this sequence. The LED was shutdown and the microcomputer read the dark signal (Sdk). Afterwards, the LED was enabled to shine, which was done by turning the variable resistor wired to the base of the transistor (Tr) (Figure 3). The intensity of the radiation beam ( $I_a$ ) was adjusted in order to allow that the photometer generated a signal ( $S_i$ ) of 2000 mV. The signal was read by the microcomputer and saved as the full-scale measurement (Fs). Since this step was carried out while maintaining the flow cell filled with carrier fluid (water), the radiation beams  $I_a$  and  $I_b$  were equal. When a sample was processed, the intensity of the radiation beam ( $I_b$ ) became less intense than the previous one, causing a decrease in the potential difference ( $S_i$ ) generated by photodetector. This signal was used for the absorbance calculation using the following equation.

$$\text{Absorbance} = \log \frac{F_s - S_{dk}}{S_i - S_{dk}} \quad (1)$$

where Sdk,  $F_s$  and  $S_i$  are the dark signal, the full-scale measurement, and the signal generated when the flow cell was filled with a sample, respectively.

The pumping flow rates were kept constant, and the variables studied were the resampling time interval ( $\Delta t_2$ ) and the concentrations of the sulfuric acid and potassium dichromate solutions. After establishing better operating conditions by modifying the length of the dispersion coil, the duration of the sampling time and the concentration of the reagent solution, samples of distilled spirits were processed using the proposed procedure and the AOAC International (Association of Official Agricultural Chemists) reference method.<sup>17</sup>

## Results and Discussions

### Effect of the resampling time

Intending to demonstrate the feasibility of the new injector, it was employed to develop a photometric procedure for the determination of ethanol in distilled spirits. Initial assays showed that when using a sampling loop with a volume of 50  $\mu\text{L}$ , the range of linear response did not reach a concentration higher than 15% (v/v) ethanol. Since the sample of interest comprised an ethanol concentration up to 45%, a sampling zone strategy was accomplished<sup>15,16</sup> by the implementation of the flow analysis module shown in Figure 4. The results obtained by varying the time interval for resampling are shown in Table 2.

It is well known that in a flow analysis system, sample is dispersed into the carrier solution during its displacement through the analytical path, generating a gradient of concentration, so that the signal generated by the detector

**Table 1.** Sequence of events to be carried out.  $V_1$  and  $V_4$  = three-way solenoid valves;  $V_2$  and  $V_3$  = pinch solenoid valves; Figure 4, I = automatic injector commutator; numbers 0 and 1 indicated the state of actuation of valves, switched off or on, respectively. The numbers in the last column at right are the selected values

Step	Event	$V_1$	$V_2$	$V_3$	$V_4$	I	time / s
1	filling reagent channel	0	1	0	0	0	20
2	washing reactor with acid solution	0	0	1	0	0	15
3	displacing injector to the injection position	0	0	0	0	1	5
4	photometer calibration	0	0	0	0	0	–
5	washing sample channel	1	0	0	0	0	20
6	displacing injector to the sampling position	0	0	0	0	1	5
7	filling sampling loop	1	0	0	0	0	10
8	displacing injector to the dilution position	0	0	0	0	1	5
9	diluting sample and emptying flow cell	0	0	0	1	0	14
10	displacing injector to the sampling position	0	0	0	0	1	5
11	addition of reagent and sample displacement for detection	0	1	1	0	0	12
12	reading signal	1	0	0	0	0	20

**Table 2.** Effect of the sampling zone time. Standard solutions of ethanol used: 0.0, 10.0, 20.0, 30.0, 40.0 and 50% (v/v). Time intervals for insertion of sample and reagent solution were both maintained at 2.0 s. Concentration of dichromate and sulfuric acid solutions were 0.2 and 4.0 mol L<sup>-1</sup>, respectively

Sampling time / s	Linear equation	Linear coefficient (r)
10	$Y = 0.0274X + 0.1913$	0.9479
12	$Y = 0.0246X - 0.0156$	0.9897
14	$Y = 0.0185X - 0.0102$	0.9953
15	$Y = 0.0179X - 0.0102$	0.9936
16	$Y = 0.0167X - 0.0101$	0.9867

presents a gaussian with an asymmetrical profile when plotted as a time function. The results shown in Table 2 were achieved by performing the resampling step (step 9, Table 1) on the descending part of the gaussian profile, which was the region of decreasing concentration. When increasing the waiting time for resampling, the angular coefficients (slope) of the linear equations are decreased, thus indicating that a portion of the sample zone that was less concentrated was collected. This effect is consistent with what is expected. Furthermore, a linearity improvement in opposition to slope can be observed. Two distinct facts leading to the same answer can be imagined: reagent insufficient to satisfy the stoichiometry of the reaction, thus resampling a more diluted sample zone compensated this effect; or saturation of the photometer took place since, for a time interval of 10 s, the calculated absorbance for a 50% ethanol solution (v/v) was higher than 1.0. These doubts were clarified with the experiments described in the next sections.

#### Effect of the reagent concentration

The experiments described earlier were performed using a potassium dichromate solution with a concentration of 0.2 mol L<sup>-1</sup>. To evaluate the effect of the concentration on the development of the reaction, a set of assays was carried out using a potassium dichromate solution with concentrations of 0.05, 0.1, 0.2 and 0.3 mol L<sup>-1</sup>. It was observed that the response was dependent on the reagent concentration. Using reagent with concentrations of 0.1 and 0.05 mol L<sup>-1</sup>, the signals generated were similar to the blank up to ethanol concentrations of 10 and 20% (v/v), respectively. The results obtained using dichromate solutions with concentrations of 0.2 and 0.3 mol L<sup>-1</sup> are shown in Figure 5, being represented by the following relationships:  $\text{Absorbance}_2 = 0.0209X + 0.0113$  ( $r = 0.9977$ ) and  $\text{Absorbance}_3 = 0.0279X + 0.015$  ( $r = 0.9938$ ) for dichromate concentrations of 0.2 and 0.3 mol L<sup>-1</sup>, respectively. The variable X represents the ethanol concentration in terms of percentage (v/v).

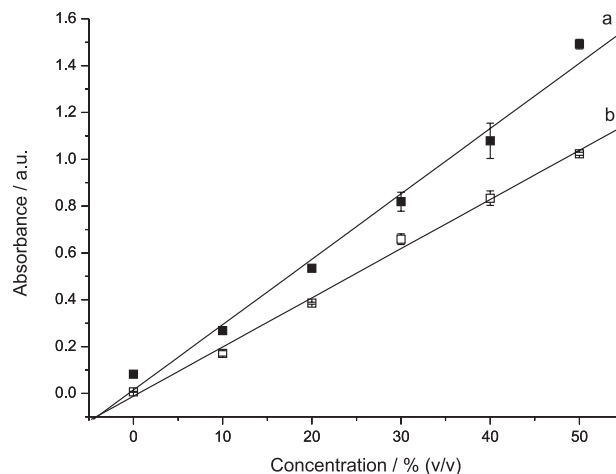


**Figure 5.** Effect of the potassium dichromate solution concentration. The curves a and b correspond to dichromate concentration of 0.3 and 0.2 mol L<sup>-1</sup>, respectively.

Since the angular coefficient (slope) of the curve for the concentration of 0.3 mol L<sup>-1</sup> is 15% higher than that obtained using the other one, it is possible to surmise that the sensitivity was dependent on the concentration of the chromogenic reagent. Nevertheless, in both cases, the procedure showed linear responses. Considering that sensitivity was not the most important factor because samples had to be diluted on line, the concentration of 0.2 mol L<sup>-1</sup> was the chosen one in order to minimize reagent consumption. The use of concentrations higher than 0.2 mol L<sup>-1</sup> generates more waste with dichromate and increases the demand for waste treatment.

#### Effect of the acidity on the signal

Ethanol was oxidized by dichromate in a sulfuric acid medium. So, in order to verify the effect of acidity on the development of the reaction, experiments were done using sulfuric acid solutions with concentrations of 2, 3, 4 and 5 mol L<sup>-1</sup>. The data shown in Table 3 indicate a sensitivity gain with increasing concentrations of sulfuric acid. Because the linearity of the calibration curve obtained with a concentration of 4 mol L<sup>-1</sup> was very good and the sensitivity was sufficient to meet the range of concentrations usually found in samples of distilled spirits, this sulfuric acid concentration was selected.

#### Effect of the dispersion coil

In this work, the sampling zone strategy was used to dilute samples exploiting the dispersion effect, which is a function of both the sampling loop and the dispersion coil lengths. The volume of the sampling loop was maintained at 50  $\mu$ L, and experiments were performed using dispersion

**Table 3.** Effect of the sulfuric acid concentration

Concentration / (mol L <sup>-1</sup> )	Linear equation	Linear coeficiente (r)
2	$Y = 0.0098X^a + 0.1292$	0.9837
3	$Y = 0.0162X^a + 0.0427$	0.9919
4	$Y = 0.0206X^a - 0.0300$	0.9949
5	$Y = 0.0367X^a - 0.0291$	0.9945

<sup>a</sup>Ethanol concentration in % (v/v).

coils (Figure 4) with lengths of 20, 30 and 40 cm. The injector waiting time in the position of dilution was programmed to vary from 1.0 to 25.0 s, in increments of 1.0 s.

The records obtained with the dispersion coil of 20 cm are shown in Figure 6, in which in the ascending part of the records, the repeatability is not good. In this case, the resampling step was performed in regions with higher gradient of concentration, so it was assumed that this feature affected the precision of the results.

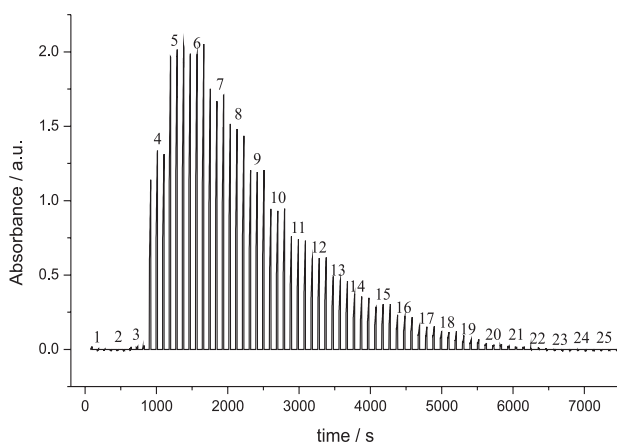


**Figure 6.** Transient signals obtained by varying the time of diluting the sample with a coil of 20 cm long. Numbers on the records refer to the time intervals presented to carry out the resampling steps. In this experiment, a solution of ethanol 30% (v/v) and a reading time of 20 s were used.

When analyzing these records, it is possible to note that the precision of the results achieved for resampling time intervals ranging from 9 to 18 s were better, therefore the appropriate time interval for resampling can be chosen within this range. The results obtained using the dispersion coils with lengths of 30 and 40 cm showed profiles similar to those in Figure 6, presenting as the main difference a wider delay time up to the record of the first signal, and a broadening band and a small attenuation on the absorbance values. These observations are consistent with those expected in a flow system based on the sampling zone approach.<sup>15,16</sup> Based on the results in Figure 6, the time interval of 14 s was selected for a sample dilution in the proposed procedure.

Considering the results discussed earlier, a set of parameters that characterize the overall performance of the proposed system was defined and is summarized in Table 4.

**Table 4.** Performance comparison

Parameter	Proposed procedure	Reference 8
Concentration range / % (v/v)	10-50	10-42
Linear equation	$Y = 0.0297X - 0.0534$	–
Linear correlation coefficient (r)	0.9972	–
Limit of detection / % (v/v)	2.0	–
Limit of quantification / % (v/v)	6.7	–
Relative standard deviation / % (RSD)	2.0	1.6
Consumption of sulfuric acid / $\mu\text{L}^a$	198	220
Consumption of sample / $\mu\text{L}^a$	50	296
Potassium dichromate consumption / $\text{mg}^a$	5.8	5.4
Effluent volume with potassium dichromate / $\text{mL}^a$	0.40	–
Total volume of effluent / $\text{mL}^a$	0.73	3.3
Sampling throughput (determination per h)	34	40

<sup>a</sup>Values are related with one determination.

The wide range of linear response is a remarkable feature, and furthermore, the reagent consumption and waste generation are very low, affording also facility in generating effluent selectively, which was done by separating the part that does not contain dichromate.

#### Determination of ethanol in distilled spirits

Intending to demonstrate the applicability of the injector and the effectiveness of the analytical procedure, the determination of ethanol in several samples of distilled spirits was carried out. In order to accomplish an accuracy assessment of the results, a set of samples was processed using a reference method, yielding the results shown in Table 5.

**Table 5.** Result comparison of ethanol in distilled spirits

Sample	Proposed procedure / % (v/v)	Reference method / % (v/v)
Cachaça 1	$36.67 \pm 0.78$	$37.88 \pm 0.03$
Cachaça 2	$49.96 \pm 0.84$	$45.64 \pm 0.04$
Cachaça 3	$34.99 \pm 0.61$	$31.20 \pm 0.01$
Cachaça 4	$40.03 \pm 0.49$	$35.88 \pm 0.02$
Cachaça 5	$38.11 \pm 0.22$	$37.88 \pm 0.02$
Whisky 1	$40.27 \pm 0.59$	$40.10 \pm 0.01$
Whisky 2	$40.15 \pm 0.76$	$38.72 \pm 0.07$

Results are average of four consecutive measurements.

To see whether there was a significant difference between the methods, the paired *t*-test was applied. The value found for 95% confidence was  $t_{\text{cal}} = 2.17$ , while the tabulated value for this level of confidence is  $t_{\text{tab}} = 2.45$ , indicating that there is no significant difference between the sets of results.

#### Features of the new injector

The results shown in the previous sections can be considered as an indication that the new version of the automatic injector worked effectively. The smaller area of friction between the movable and static parts allowed the use of a small DC motor to displace the central bar in order to carry out the sampling and injection steps. The time interval to displace the movable part between the commuting positions was 3.5 s, which could be considered long compared with the earlier version that was moved using two solenoids.<sup>6</sup> While the displacing of the central part was in course, the flow lines were blocked, thus to avoid over pressure and fluid leakage, all valves were shot down (Figure 4). This time interval can be decreased employing a motor with rotation higher than 17 rpm. While the earlier version employed two solenoid with 10 W of power, the new version employed a DC motor of 4.8 W. Both devices can be controlled using same electronic interface, thus the new version presented advantage concerning energy consumption.

In the earlier version of the injector, the tubes used as flow lines were attached using as fitting pieces of Tygon tubing glued to injector parts. In the new version, the flow lines were attached using ring-seal of rubber that facility the removing for maintenance. The maintenance of the injector movable part was carried out weekly lubricating with silicon grease.

#### Conclusion

The results obtained show that the proposed injector may be used as an alternative to conventional one. Its robustness was ascertained by using it for six months with no need of replacing any part, excepting the silicon rubber strip rubber glued onto the movable part of the injector that was replaced only once. The results obtained by analyzing samples of distilled spirits demonstrated the effectiveness of the proposed device, thus indicating that it can be considered a reliable tool for the development of automatic analytical procedures. In addition, the proposed flow analysis module associating the automatic injector to a set of solenoid valves added the advantages of reducing

reagent consumption and the generation of effluent, and also allowing the selective generation of effluents with and without dichromate. Therefore, it is possible to conclude that the proposed system, as a whole, aggregated advantages over previously proposed procedure,<sup>8</sup> especially in the case of waste generation.

#### Acknowledgements

The authors acknowledge financial support from CNPq, CAPES, FAPESP and INCTAA.

#### References

1. Ruzicka, J.; Hansen, E. E.; *Anal. Chim. Acta* **1975**, *78*, 145.
2. Stewart, J. W. B.; Ruzicka, J.; Bergamin Filho, H.; Zagatto, E. A.; *Anal. Chim. Acta* **1976**, *81*, 371.
3. Ruzicka, J.; Hansen, E. H.; Mosbaek, H.; Krug, F. J.; *Anal. Chim. Acta* **1977**, *49*, 1858.
4. Bergamin, N.; Medeiros, J. X.; Reis, B. F.; Zagatto, E. A. G.; *Anal. Chim. Acta* **1978**, *101*, 9.
5. Bergamin, H.; Reis, B. F.; Jacintho, A. O.; Zagatto, E. A. G.; *Anal. Chim. Acta* **1980**, *117*, 81.
6. Martelli, P. B.; Reis, B. F.; Korn, M.; Rufini, I. A.; *J. Braz. Chem. Soc.* **1997**, *8*, 479.
7. Raimundo, I. M.; Pasquini, C. *Analyst* **1997**, *122*, 1039.
8. Comitre, A. L. D.; Reis, B. F.; *Lab. Robot. Autom.* **2000**, *12*, 31.
9. Choengchan, N.; Mantima, T.; Wilairata, P.; Dasgupta, P. K.; Motomizub, S.; Nacaprich, D.; *Anal. Chim. Acta* **2006**, *579*, 33.
10. Reis, B. F.; Gine, M. F.; Zagatto, E. A. G.; Lima, J. L. F. C.; Lapa, R. A.; *Anal. Chim. Acta* **1994**, *293*, 129.
11. Melchert, W. R.; Reis, B. F.; Rocha, F. R. P.; *Anal. Chim. Acta* **2012**, *714*, 8.
12. Freitas, S. K. B.; Silva, V. L.; Araujo, A. N.; Montenegro, M. C. B. S. M.; Reis, B. F.; Paim, A. P. S.; *J. Braz. Chem. Soc.* **2011**, *22*, 279.
13. Zárate, N.; Perez-Olmos, R.; Reis, B. F.; *J. Braz. Chem. Soc.* **2011**, *22*, 1009.
14. Borges, S. S.; Peixoto, J. S.; Feres, M. A.; Reis, B. F.; *Anal. Chim. Acta* **2010**, *668*, 3.
16. Rocha, F. R. P.; Martelli, P. B.; Frizzarin, R. M.; Reis, B. F.; *Anal. Chim. Acta* **1998**, *366*, 45.
17. Cunniff, P.; *Official Methods of Analysis of AOAC International*, 16<sup>th</sup> ed.; AOAC International: Arlington, USA, 1995.

Submitted: October 1, 2012

Published online: May 24, 2013

FAPESP has sponsored the publication of this article.